Molecular Therapy
Nucleic Acids
Original Article

ssODN-Mediated In-Frame Deletion with CRISPR/Cas9 Restores FVIII Function in Hemophilia A-Patient-Derived iPSCs and ECs

Zhiqing Hu,[1] Miaojin Zhou,[1] Yong Wu,[1] Zhuo Li,[1] Xionghao Liu,[1] Lingqian Wu,[1] and Desheng Liang[1]

[1]Center for Medical Genetics, School of Life Sciences, Central South University, Changsha, Hunan 410078, China

Given that the cDNA of *F8* is too large to be packaged into adeno-associated virus (AAV) capsids, gene transfer of some versions of B-domain-deleted *F8* (BDD-*F8*) for hemophilia A (HA) treatment has been attempted with promising results. Here, we describe an efficient gene correction via single-stranded-oligodeoxynucleotide (ssODN)-mediated in-frame deletion within the B domain of *F8* with CRISPR/Cas9 in HA-patient-derived induced pluripotent stem cells (HA-iPSCs). The expression and activity of FVIII was restored in corrected HA-iPSC-derived induced endothelial progenitor cells (C-iEPCs) *in vitro* and *in vivo*. The bleeding phenotype was rescued in HA mice after C-iEPC infusion. Our results demonstrate an efficient approach for *in situ* gene correction via introduction of a tiny deletion using ssODN and CRISPR/Cas9 to reframe the *F8* transcript and restore FVIII function in HA-iPSC-derived EPCs with potential clinical impact in HA gene therapy. For the first time, we demonstrated *in vitro* and *in vivo* the FVIII function that is encoded by the endogenous *F8* gene with a partially deleted B domain. This work also suggests an applicable strategy for genetic correction of other gene frameshift mutations.

INTRODUCTION

Hemophilia A (HA) is an X-linked recessive genetic bleeding disorder (incidence of 1 in 5,000 male births).[1] It is caused by genetic mutations in human coagulation factor 8 (*F8*). The Human Gene Mutation Database (HGMD)[2] reports 3,246 mutations (475 in the B domain) of *F8* that cause HA. Approximately 90.7% of the B domain mutations result in premature termination.

Traditionally, HA is treated by replacement therapy with repeated infusions of plasma-derived or recombinant factor VIII (FVIII) protein. However, antibody formation and the high cost of repeated infusions limit this method. Gene therapy is a promising option for curing hemophilia. *In vivo* gene therapy for hemophilia B (HB) has shown therapeutic effects in clinical trials using a recombinant adeno-associated viral (rAAV) vector carrying the *F9* gene.[3] For gene therapy for HA, which accounts for 80%–85% of all hemophilia cases, the *F8* cDNA (7 kb) is too large for packaging into the AAV capsids. Approaches using B-domain-deleted *F8* (BDD-*F8*) have been tested, with some having shown therapeutic effects in animal models[4] and some having proceeded to clinical trials.[5] However, the potential for immune responses, transduction of nontarget cells, and random insertional mutagenesis continues to hinder its clinical application.[6] On the other hand, as genome editing is emerging as an ideal approach for manipulation of genes *in situ*, studies have focused on *ex vivo* gene therapy for HA after targeted genetic modification of pluripotent stem cells, including *in situ* gene correction,[7] reversion[8,9] for the *F8* inversion mutations, and ectopic integration of BDD-*F8* at the rDNA locus,[10] some of which have been shown to restore FVIII function in cells or in HA mice.

The CRISPR/Cas9 system has been used for genome editing, including chromosomal segment deletion,[11] elimination,[12] rearrangement,[13,14] and precise gene mutations.[15,16] Combination of CRISPR/Cas9 with single-stranded oligodeoxynucleotide (ssODN) has been shown to be efficient at inducing gene addition and precise gene mutation.[17,18] However, there has been no report on ssODN-mediated precise deletion with CRISPR/Cas9, whereas efficient ssODN-mediated targeted gene deletion with transcription-activator-like effector nucleases (TALENs) has been described.[19]

Because of its unlimited proliferation ability and multidirectional differentiation potential, induced pluripotent stem cells (iPSCs) have become ideal targets for *ex vivo* gene therapy. Liver sinusoidal endothelial cells (LSECs) are highly specialized endothelial cells (ECs) that produce and secret FVIII in humans.[20,21] ECs express von Willebrand factor (vWF), which is stored in Weibel-Palade bodies as a carrier protein to stabilize FVIII.[22] Studies have shown that iPSC-derived endothelial progenitor cells (iEPCs) are integrated into liver sinusoids after intrahepatic injection in mice, resulting in therapeutic levels of FVIII production.[23]

Received 6 November 2018; accepted 27 May 2019;
https://doi.org/10.1016/j.omtn.2019.05.019.

Correspondence: Desheng Liang, MD, PhD, Center for Medical Genetics, School of Life Sciences, Central South University, 110 Xiangya Road, Changsha, Hunan 410078, China.
E-mail: liangdesheng@sklmg.edu.cn
Correspondence: Dr. Lingqian Wu, MD, PhD, Center for Medical Genetics, School of Life Sciences, Central South University, 110 Xiangya Road, Changsha, Hunan 410078, China.
E-mail: wulingqian@sklmg.edu.cn

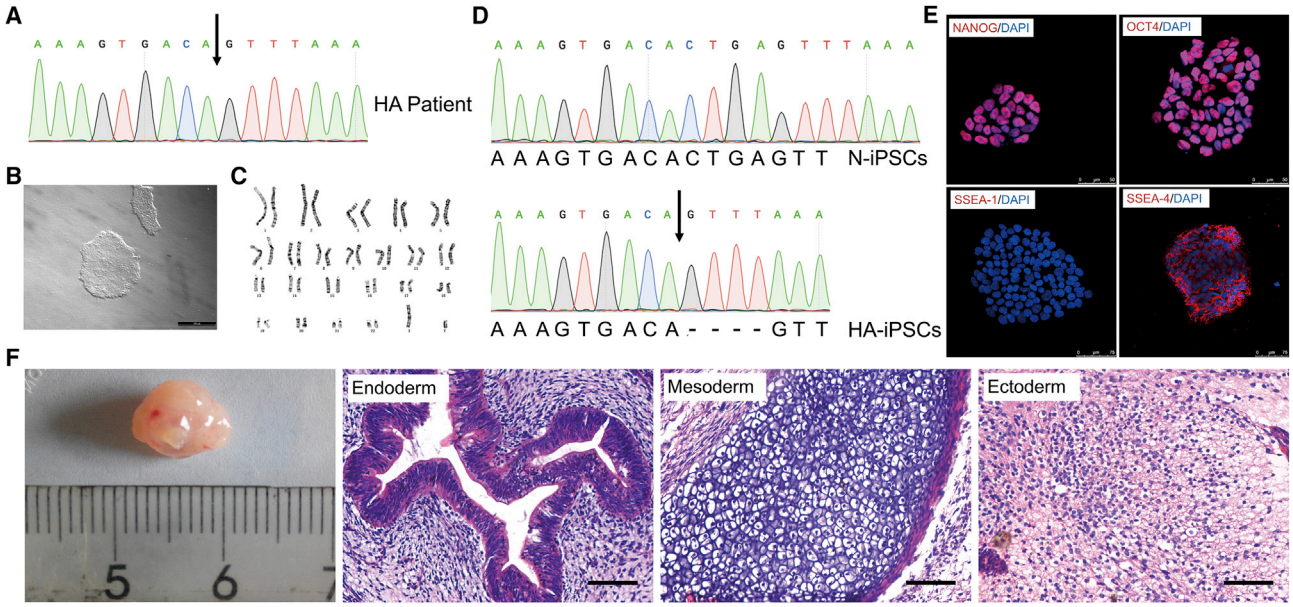

Figure 1. Generation and Characterization of c.3167del CTGA HA-iPSCs

(A) Molecular diagnosis of the *F8* frameshift mutation c.3167del CTGA using Sanger sequencing. The arrow indicates the location of the deletion. (B) Bright field image of a representative iPSC clone. Scale bar, 500 μm. (C) Karyotyping of HA-iPSCs is shown. (D) Sanger sequencing analysis of HA-iPSCs. N-iPSCs were used as the normal control. (E) Immunofluorescence showed that iPSCs expressed the markers NANOG, OCT4, and SSEA-4 and did not express the differentiation marker SSEA-1. (F) H&E staining of a teratoma derived from HA-iPSCs that included three germ layers: endoderm (respiratory epithelium), mesoderm (cartilage), and ectoderm (neural tissue). Scale bar, 50 μm.

In this study, to avoid invasive sampling, urine cells were isolated from a patient with severe HA (4-bp frameshift deletion of the B domain in exon 14 of *F8*, which resulted in premature termination of translation), and reprogrammed into iPSCs (HA-iPSCs). Using CRISPR/Cas9 and ssODN, we achieved an efficient reframing of the 4-bp frameshift deletion via targeted deletion of 50 bp within the *F8* B domain in HA-iPSCs. FVIII expression and activity were demonstrated in reframed iPSC-derived EPCs (iEPCs) *in vitro* and *in vivo*.

RESULTS

Generation and Characterization of HA-iPSCs

First, we genotyped and identified an *F8* frameshift mutation of c.3167del CTGA in a 21-year-old male patient with severe HA (Figure 1A). Given that invasive biopsy should be avoided in bleeding disorders, and isolation of urinary cells is simple, cost-effective, and universal,[24] we collected urine samples from the patient to expand the urine cells. The urine cells appeared cobblestone-like (Figure S1) and expressed markers of renal tubular epithelial cells, zonula occludens-protein 1 (ZO-1), intermediate filament keratin 7 (KRT7), and β-catenin (Figure S1). These results are consistent with those described in previous reports on the cultivation of human renal tubular epithelial cells from the urinary tract and the renal tubular system.[25,26] We then generated HA-iPSCs from the renal tubular epithelial cells using retroviral vectors carrying four Yamanaka factors (OCT4, Sox2, Klf4, and c-Myc).[25,27] After induction, the human embryonic stem cell (ESC)-like clones were isolated for further characterization (Figure 1B). We examined the pluripotency and genetic stability of the iPSC line, using immunofluorescence, teratoma formation, and karyotyping. The results showed that the HA-iPSCs were karyotypically normal (Figure 1C) and maintained the mutated genotype. Normal iPSCs (N-iPSCs) purchased from ATCC were used as a control (Figure 1D). The HA-iPSCs expressed OCT4, NANOG, and stage-specific embryonic antigen (SSEA)-4, but did not express SSEA-1, which was consistent with the expression observed in human ESCs (hESCs) (Figure 1E). Spontaneous differentiation in the center of the HA-iPSC colony was occasionally observed during iPSCs maintenance, as it is in hESCs. The HA-iPSCs formed teratomas *in vivo* that contained all three germ layers, including respiratory epithelium (endoderm), cartilage tissue (mesodermal), and neuroepithelial tissue (ectoderm) (Figure 1F).

CRISPR/Cas9 and ssODN-Mediated Targeted Deletion in *F8* of HA-iPSCs

CRISPR/Cas9 and ssODN were used to create an in-frame deletion. The designation of single-guide RNA (sgRNA) is restricted by the protospacer adjacent motif (PAM) sequence. In this case, the minimal deletion that could be achieved is 54 bp, including the 4-bp frameshift deletion of the B domain in exon 14 of the *F8* gene (Figure 2A). The nearest dual-sgRNAs mapping to the target sites were designed,[28] constructed, and verified to possess cleavage activity via sequencing and the T7 endonuclease I (T7E1) assay (Figure S2; Table S1). The cleavage activities of F8-E14-sg1 and F8-E14-sg2 were 41.30% and 18.92%, respectively (Figure 2B). The corresponding ssODN template

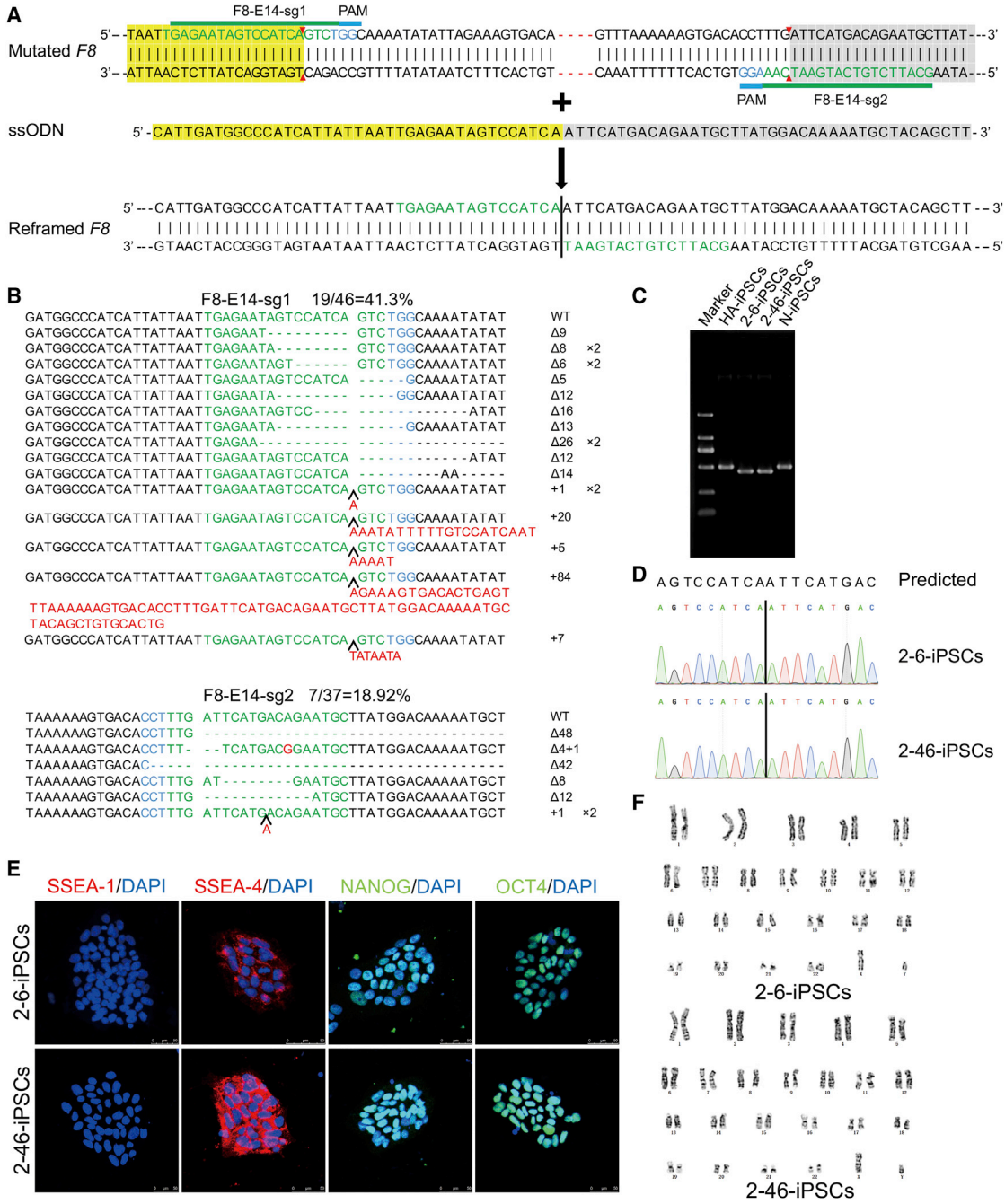

Figure 2. Generation of Corrected HA-iPSCs Mediated by ssODN with CRISPR/Cas9

(A) Schematic representation of CRISPR/Cas9-mediated precise deletion. The design of two sgRNAs for *F8* exon 14 was shown. The red dotted line indicates c.3167del CTGA. Green letters indicate the sgRNA sequences, and blue letters indicate the protospacer adjacent motif (PAM). The red arrow represents the predicted CRISPR/Cas9 cleavage sites. The reframed *F8* exhibits a precise 50-bp deletion and correction of the reading frame of frameshift mutations in this region. The vertical line indicates the upstream and downstream connections. Yellow-shaded bases are left homologous sequences, and gray-shaded bases are right homologous sequences. (B) Sanger sequencing of the indels induced by F8-E14-sg1 or F8-E14-sg2 in HA-iPSCs. WT, wild-type; Δ, deletion; +, insertion; ×, times. The black arrow indicates the position of insertion. The blue-labeled bases are the PAM sequences of CRISPR/Cas9, the target sequence of sgRNA is shown in green, and red indicates inserted bases. (C) PCR-based screening of C-iPSCs. The sizes of the PCR products were 448 bp for the 50-bp deletion, 502 bp for the N-iPSCs, and 498 bp for the HA-iPSCs, amplified using the primer pair F8-E14-F/R. (D) The PCR products were sequenced by Sanger sequencing. (E) Each C-iPSC line (2-6-iPSCs and 2-46-iPSCs) expressed SSEA-4, NANOG, and OCT4 and did not express SSEA-1, as determined by immunofluorescence. DAPI was used for nuclear staining. (F) Karyotypes of C-iPSC (2-6-iPSC and 2-46-iPSC) lines are shown.

Table 1. Potential Off-Target Sites with up to Five Mismatches Identified by CAS-OFFinder

Target Sequence	Mismatch	Number of Targets Identified
GGCATTCTGTCATGAATCAANRG	1	1
GGCATTCTGTCATGAATCAANRG	2	3
GGCATTCTGTCATGAATCAANRG	3	26
GGCATTCTGTCATGAATCAANRG	4	329
GGCATTCTGTCATGAATCAANRG	5	3,125
GTGAGAATAGTCCATCAGTCNRG	3	11
GTGAGAATAGTCCATCAGTCNRG	4	150
GTGAGAATAGTCCATCAGTCNRG	5	1,803

Table 2. Variants of iPSCs Identified Using WES

Clone	HA-iPSCs	2-6-iPSCs	2-46-iPSCs
All variants	31,245	30,842	31,381
All indels	1,741	1,655	1,750
Reframed clone-specific indels	N/A	167	189
Possible off-target sites after alignment with predicted off-target sites	N/A	0	0

N/A, not applicable.

was synthesized directly by Sangon Biotech. To perform gene targeting, plasmids expressing sgRNAs and the CRISPR/Cas9 complex and ssODN were nucleofected into the HA-iPSCs. After nucleofection with CRISPR/Cas9 and ssODN, the HA-iPSCs were dissociated into single cells, plated on murine embryonic fibroblast (MEF) feeder cells without drug selection, and then picked and expanded. These clones were initially screened via PCR. Then, the *in situ* gene-corrected iPSCs (C-iPSCs) were verified by Sanger sequencing. Of the 34 analyzed clones, 5 were identified as the corrected clones, indicating high targeting efficiency (14.7%) without screening, but only 1 positive clone was found among the 48 clones in the non-ssODN group (Table S2). We randomly selected two stably corrected clones—2-6-iPSC and 2-46-iPSC—for further research, in which the targeted deletion of 50 bp was verified by PCR (Figure 2C) and Sanger sequencing (Figure 2D). In addition, the 2-6-iPSCs and 2-46-iPSCs were shown to be pluripotent by immunofluorescence (Figure 2E) and were karyotypically normal (Figure 2F). Spontaneous differentiation in the center of the C-iPSC colony was observed during iPSC maintenance, as in the HA-iPSCs. The percentage of differentiated colonies was lower than 5% in the HA-iPSCs, N-iPSCs, and C-iPSCs, as more than 95% of the cell population was positive for the stem cell marker OCT4. A premature *F8* mRNA was detected, indicating that there was no nonsense-mediated mRNA decay (NMD) of the reframed mRNA in the HA-iPSCs and C-iPSCs (Figure S3A), which is consistent with a previous report.[29] FVIII expression was detected in cell lysates, but almost none was detected in the supernatant of the HA-iPSCs, C-iPSCs, and N-iPSCs via ELISA, indicating that FVIII was not secreted at the iPSC stage (Figure S3B). It has been reported that the complex formed by lectin mannose-binding 1 (LMAN1) and multiple coagulation factor deficiency 2 (MCFD2) mediates the secretion of FVIII, and mutation of *LMAN1* or *MCFD2* leads to a lack of both FV and FVIII.[30] We detected LMAN1 by western blot analysis and found that the LMAN1 protein was absent in human iPSCs but was expressed in human iECs (Figure S3C), indicating that there was no secretion of FVIII at the iPSC stage.

No Off-Target Sites Were Observed Among the Predicted Sites in C-iPSCs

To analyze the off-target activity of CRISPR/Cas9, genomic DNA was isolated from the HA-iPSCs and C-iPSCs (2-6-iPSCs and 2-46-iPSCs). We selected and designed primers to amplify the five potential off-target sites for F8-E14-sg1 and F8-E14-sg2, respectively, that were predicted by the Optimized CRISPR Design website (Tables S3, S4, and S5).[28] Then, the DNA of the C-iPSCs was amplified by PCR and sequenced, and no indels were observed upon comparison with the HA-iPSCs (Figures S4 and S5). Meanwhile, unintended mutations after CRISPR/Cas9 editing in the C-iPSCs (2-6-iPSCs and 2-46-iPSCs) were investigated by comparison with the HA-iPSCs, using whole-exome sequencing (WES). We focused on indels rather than single nucleotide variants (SNVs) based on the finding that programmable nucleases rarely generate point mutations.[31,32] First, we identified indels in the C-iPSCs but not in the HA-iPSCs; there were 167 unique indels in the 2-6-iPSCs and 189 in the 2-46-iPSCs. Next, potential off-target sites for mismatches with on-target sites of CRISPR/Cas9 of up to five nucleotides (Table 1) were searched for by using Cas-OFFinder (http://www.rgenome.net/).[32] Finally, no off-target indels were identified upon comparison of the potential off-target sites with the indel locations identified by WES (Table 2). Consistent with a previous report,[33] these results indicated that there were no indel off-target mutations caused by CRISPR/Cas9 in the C-iPSCs in this study.

FVIII Expression Was Restored in C-iPSC-Derived ECs

The 50-bp targeted deletion was expected to reframe the 4-bp frameshift deletion in the *F8* B domain and restore the function of the FVIII protein. Because human ECs can secrete FVIII, the C-iPSCs (2-6-iPSCs and 2-46-iPSCs), HA-iPSCs, and N-iPSCs were differentiated into C-iECs, HA-iECs, and N-iECs (Figure 3A) via the optimized OP9 coculture method, to examine the recovery of FVIII secretion.[34] A deleted *F8* transcript was detected, indicating that there was no NMD of the 54-bp deletion mRNA in the C-iECs (2-6-iECs and 2-46-iECs) (Figure 3B). ELISA results showed that FVIII secretion in the C-iECs (2-6-iECs and 2-46-iECs) was higher than that in the C-iPSCs, similar to that in the N-iECs, and higher than that in the HA-iECs (Figure 3C). Meanwhile, FVIII activity was measured in the culture supernatant of the C-iECs (2-6-iECs and 2-46-iECs), but not in that of the HA-iECs (Figure 3D), indicating that FVIII function was restored in the C-iECs.

Restoration of FVIII Expression and Secretion in C-iPSC-Derived EPCs

Using a previously described method,[35] we differentiated C-, HA-, and N-iPSCs into C-iEPCs, HA-,iEPCs and N-iEPCs via small-molecule-mediated activation of WNT signaling; flow cytometric analysis

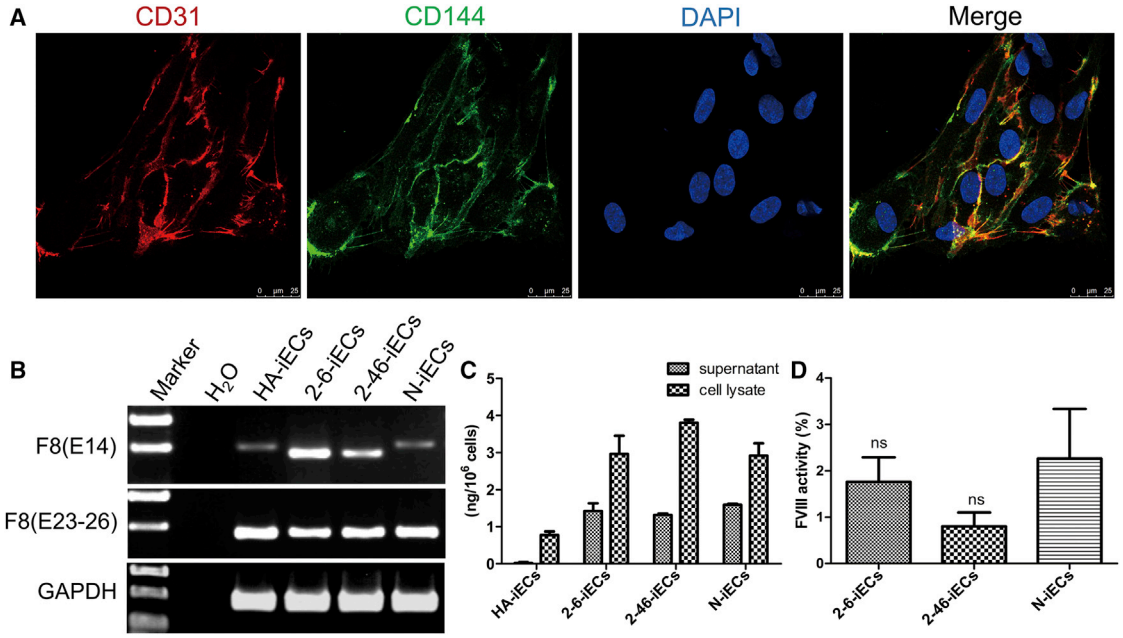

Figure 3. Restoration of FVIII Expression in C-iECs

(A) Immunofluorescence staining of iECs expressing markers for CD31 (red) and CD144 (green). DAPI was used to visualize the nucleus. (B) RT-PCR analysis of *F8* expression in iECs. Primers based on exon 14 (E14) and primers based on exons 23 and 26 (E23–E26) were used to detect *F8* expression. *GAPDH* was used as a loading control. (C) FVIII antigen levels in ECs derived from iPSCs were measured by ELISA. Bars represent the mean ± SEM (n = 3, independent cultures). (D) FVIII activity in the supernatants of differentiated ECs. The FVIII activity of the HA-iECs was lower than the detection limit of the instrument. No significant difference in FVIII activity was observed between C-iECs (2-6-iECs and 2-46-iECs) and N-iECs. Bars represent the mean ± SEM (n = 3, independent cultures). ns, not significant, compared with N-iECs.

showed that the differentiation efficiency was between 10% and 20% (Figure 4A). The iEPCs were sorted by a CD31 microbead-based antibody; characterized using immunostaining of CD34 (sc-74499; Santa Cruz), CD31 (P8590l; Sigma-Aldrich), and CD144 (ab33168; Abcam) (Figure 4B); and functionally verified by angiogenesis (Figure S6A) and Dil-acetylated-low-density-lipoprotein (Dil-AcLDL) endocytosis (Figure S6B). RT-PCR was used to distinguish the premature *F8* transcript from the 4-bp-deleted *F8*, indicating that there was no NMD in the HA-iEPCs (Figure 4C). ELISA results showed that the 2-6- and 2-46-iEPCs secreted FVIII at levels of 1.21 ng/10^6 cells and 0.66 ng/10^6 cells, respectively, which were higher than the levels in the HA-iEPCs (0.24 ng/10^6 cells) and similar to those in the N-iEPCs (0.46 ng/10^6 cells) (Figure 4D). After cultivation for 1 week, the sorted iEPCs expressed vWF (ab6994; Abcam), indicating that mature iECs were formed from the iEPCs (Figure 4E). FVIII in the C-iECs (2-6-iECs and 2-46-iECs) and the N-iECs was detected by both an N-terminal FVIII antibody (sc-27649; Santa Cruz) (Figure 4F) and a C-terminal FVIII antibody (ESH-8; Sekisui Diagnostics) (Figure 4G), whereas the truncated FVIII in the HA-iEPCs was detected by only the N-terminal FVIII antibody (Figure 4F).

Rescue of FVIII Deficiency and the Bleeding Phenotype Via C-iEPC Transplantation in HA Mice

To validate the therapeutic effects *in vivo*, HA-iEPCs, C-iEPCs (2-6-iEPCs and 2-46-iEPCs), and N-iEPCs were infused into HA mice via the retro-orbital vein. Two weeks after infusion, a tail-clip assay was performed, as previously described[9]; the evaluation duration of the tail-clip challenge experiment is 48 h. All the untreated HA mice (n = 9), as well as those receiving transplanted HA-iEPCs (n = 9), died soon after the tail-clip challenge (Figure 5A). The average survival time was 5.73 h (range, 1.97–10.67 h) and 5.42 h (range 1.66–8.38 h), respectively (Figure 5B). Although the average survival time in HA mice treated with the cells derived from the C-iPSCs (2-6-iEPCs and 2-46-iEPCs) was 16.83 h (range, 7.67–29.50 h) and 15.70 h (7.47–30.63 h), which exhibited a significant increase compared to non-treated HA mice (Figure 5B). Notably, 4 of the 12 HA mice with 2-6-iEPCs and 4 of the 10 HA mice with 2-46-iEPCs were alive 2 days after the tail-clip challenge, which was the endpoint of this experiment. Then, the mouse plasma was collected and assayed for FVIII activity, which is reported here as a percentage of the activity in wild-type mice. The FVIII activity in HA mice with C-iEPCs was 12.74% and 14.09%, which was significantly higher than that in HA mice (6.41%) (Figure 5C). The livers of the mice with 2-46-iEPCs that survived the challenge were collected on day 7 after the tail-clip challenge (liver collection was performed during week 3 after the 2-46-iEPC injection) to detect human cells by using immunofluorescence, and the results showed that anti-human vWF-positive cells homed to the livers of HA mice injected with 2-46-iEPCs but not in livers of HA mice with Dulbecco's phosphate-buffered saline (DPBS). Liver collection was performed during week 2 after DPBS injection.

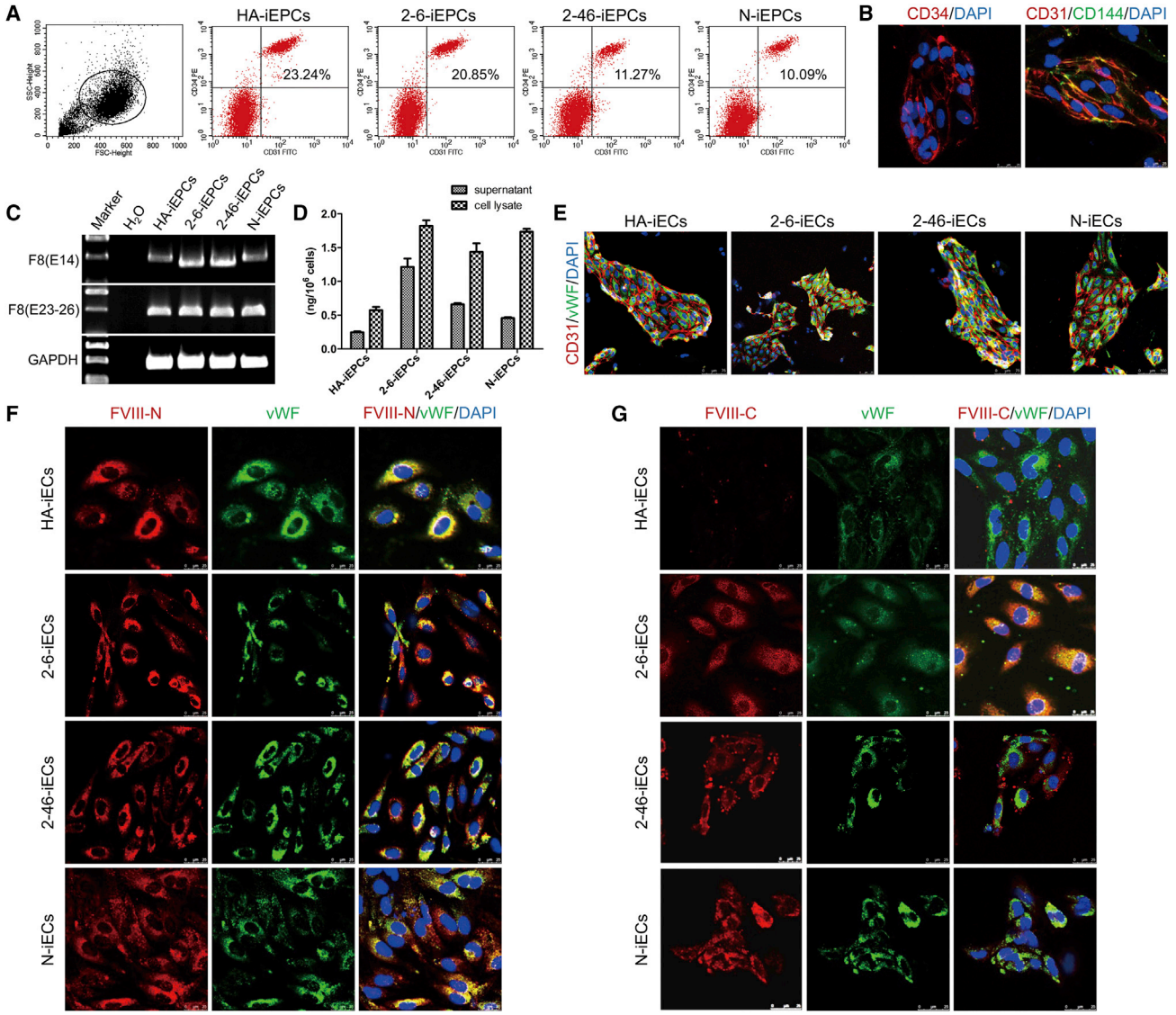

Figure 4. FVIII Expression Was Restored in C-iPSC-Derived EPCs

(A) FACS analysis of the expression of the iEPC markers CD31 and CD34 on day 5 after differentiation. (B) Immunofluorescence staining of CD34 (red), CD31 (red), and CD144 (green) in C-iEPCs. Scale bar, 25 μm. (C) RT-PCR analysis of *F8* expression in iEPCs. Primers based on exon 14 (E14) and primers based on exons 23 and 26 (E23–26) were used to detect *F8* expression. *GAPDH* was used as a loading control. (D) FVIII antigen in iEPCs differentiated from hiPSCs was detected by ELISA. Bars represent the mean ± SEM (n = 3, independent cultures). (E) Immunostaining of endothelial markers CD31 and vWF in the mature iECs from iEPCs. (F and G) *F8* expression in mature ECs derived from HA-iPSCs (HA-iECs), C-iPSCs (2-6-iECs and 2-46-iECs), and normal controls (N-iECs) was detected via immunostaining by an (F) N-terminal or (G) C-terminal FVIII antibody. DAPI was used for nuclear staining. FVIII-N, F8 protein, N-terminal. FVIII-C, F8 protein, C-terminal. Scale bar, 25 μm.

(Figures 5D and 5E). Anti-human vWF-positive cells were also detected in the lungs, but not in the spleens, hearts, kidneys, or brains of HA mice with 2-46-iEPCs (Figure 5E).

DISCUSSION

The function of the B domain of the *F8* gene remains unclear.[36] Previous studies have suggested that the *F8* B domain is associated with intracellular synthesis,[37] secretion,[38–40] activation,[41,42] inactivation,[43] and clearance[44] of FVIII. However, recombinant B domain-deleted FVIII (BDD-FVIII) has been demonstrated to be effective in clinical applications.[45,46] Gene addition of BDD-*F8* cDNA rescued the phenotype in HA model mice,[47,48] and a phase I/II clinical trial demonstrated the effectiveness of AAV5-BDD-F8 gene transfer.[5] In the present study, a 4-bp frameshift deletion within the B domain in exon 14 of *F8* resulted in premature termination of FVIII translation or FVIII truncation, leading to a severe phenotype in the patient.

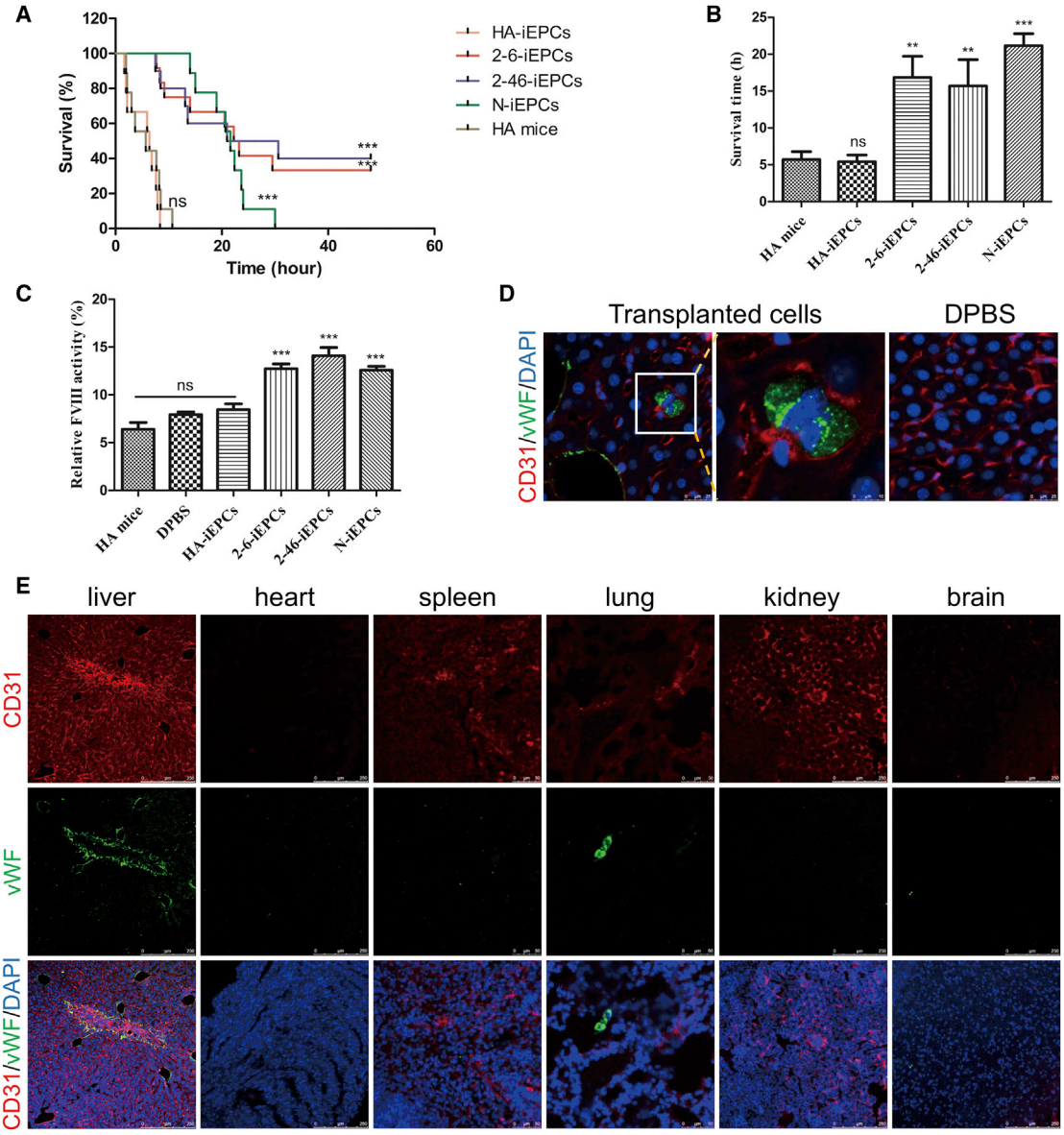

Figure 5. Functional Rescue of FVIII Deficiency in HA Mice by C-iEPCs

(A) Proportions of surviving mice after the tail-clip challenge. HA mice, mice with hemophilia A (n = 9); HA-iEPCs, mice with hemophilia A, receiving transplanted cells derived from HA-iPSCs (n = 9); 2-6-iEPCs, mice with hemophilia A, receiving transplanted cells derived from 2-6-iPSCs (n = 12); 2-46-iEPCs, mice with hemophilia A, receiving transplanted cells derived from 2-46-iPSCs (n = 10); N-iEPCs, mice with hemophilia A, receiving transplanted cells derived from N-iPSCs (n = 9). ns, not significant compared with HA mice; ***$p < 0.001$ compared with the HA-iEPC group (log-rank test). (B) Average survival time of mice after the tail-clip challenge. Notably, 4 of the 12 HA mice that received 2-6-iEPC transplants and 4 of the 10 HA mice that received 2-46-iEPC transplants and survived the challenge were excluded from this analysis. Bars represent the mean ± SEM; ns, not significant compared with HA mice. ***$p < 0.001$ and **$p < 0.01$ compared with the HA-iEPCs. (C) Relative FVIII activity was determined in plasma from HA mice with no transplant (n = 6) and HA mice with a transplant of Dulbecco's phosphate-buffered saline (DPBS) (n = 6), HA-iEPCs (n = 6), N-iEPCs (n = 8), or C-iEPCs (2-6-iEPCs and 2-46-iEPCs) (n = 8). Bars represent the mean ± SEM. ***$p < 0.001$ compared with HA-iEPCs. (D) Livers of HA mice with 2-46-iEPCs that survived the tail-clip challenge were collected and analyzed using tissue immunofluorescence with an anti-human vWF antibody, and the results indicated that the transplanted human cells homed to the mouse liver. No signal was detected in the negative control (DPBS) group. CD31 (red); vWF (green). DAPI was used for nuclear staining. (E) Tissue immunofluorescence analysis of main organs of mice with 2-46-iEPCs, showing that anti-human vWF-positive cells were detected in the livers and lungs, but not in the spleens, hearts, kidneys, or brains. CD31 (red); vWF (green). DAPI was used for nuclear staining.

Theoretically, in-frame deletion (in multiples of 3) of base pairs that include the 4-bp deletion within the B domain will reframe the *F8* frameshift mutation and restore FVIII function. We therefore precisely induced a 54-bp deletion that included the intrinsic 4-bp deletion within the B domain to reframe the *F8* open reading frame (ORF) in HA-iPSCs using ssODN and CRISPR/Cas9. FVIII expression and secretion were restored in C-iECs and C-iEPCs, and FVIII activity and the bleeding phenotype were rescued in HA mice after transplantation of C-iEPCs. Our findings indicated that deletion of 54 bases (18 amino acids) in the B domain did not affect FVIII function. We used the Swiss Model to predict protein structure,[49,50] showing that the predicted N-terminal and C-terminal structures of the FVIII protein from the 54-bp-deleted *F8* gene were both identical to those of the wild-type FVIII protein, further supporting the effectiveness of our strategy.

HA has long been identified as an ideal target for gene therapy because 1%–5% of normal plasma FVIII can significantly improve the quality of life of patients. *In situ* gene correction enables expression of the corrected gene under the regulation of endogenous promoter and *cis*-acting elements.[51,52] Some studies[53,54] have shown that knocking out some exons of the *DMD* gene in iPSCs derived from Duchenne muscular dystrophy (DMD) patients effectively reduced DMD phenotypes at the cellular and whole-mouse levels. In this study, our strategy to reframe a frameshift mutation by deleting some tiny sequence was not only an effective *in situ* genetic repair mechanism, but also greatly improved the targeting efficiency, exhibiting potential for future *in vivo* applications. Although it addresses only specific cases, this study provides a reference for the repair of other gene mutations that lead to premature termination of translation, further expanding the range of applications.

The human LSEC is the main cell type that produces and secretes FVIII.[20,21] For HA therapy, transplantation of mature murine LSECs into HA mice via the portal vein has been reported to improve FVIII activity.[55] Mature ECs cannot proliferate to maintain long-term therapeutic effects *in vivo* after cell transplantation. Given that EPCs can either proliferate or mature into ECs that secrete FVIII and that no tumorigenesis from adult EPCs engraftments has been reported,[56,57] EPCs are clearly a promising cell type for *ex vivo* HA therapy. In addition, human leukocyte antigen (HLA) matching is very strict for EPCs; therefore, transplantation of autologous EPCs and/or ECs as individualized treatments also leads to satisfactory therapeutic effects in clinical applications.[58] In the present study, we intravenously infused C-iEPCs into HA mice and demonstrated therapeutic effectiveness *in vivo*. Interestingly, the infused human iEPCs exhibited homing to the livers of mice. Although the number of homed C-iEPCs was relatively small, the bleeding phenotype in HA mice was rescued, which was consistent with a previous report in which substantial levels of human factor IX (hFIX) were obtained, even though hF9 mRNA accounted for a small fraction (0.5%) of the total wild-type mouse albumin (mAlb) transcript.[59]

MATERIALS AND METHODS

Generation of HA-iPSCs

Sterile urine was collected from a 21-year-old male patient who was diagnosed with severe HA. Cells from the urine sample were isolated and expanded. Briefly, after centrifugation at 170 × *g* for 10 min at room temperature, the urine sample was washed twice with DPBS, and the cells from the urine sample were plated on gelatin-coated 12-well plates using primary medium (DMEM/F12 supplemented with 10% fetal bovine serum [FBS]; SingleQuot Kit; Lonza, Alpharetta, GA, USA) and 1% penicillin-streptomycin). After 4 days of cultivation with primary medium, the urine cells were expanded in renal epithelial basal medium (Lonza) supplemented with Renal Epithelial Growth Medium (REGM) from the SingleQuot Kit. The urine cells were stained with β-catenin (BD Transduction Laboratories, Lexington, KY, USA), KRT7 (Gene Tex, Irvine, CA, USA), and ZO-1 (Thermo Fisher Scientific, Waltham, MA, USA). The cells were then reprogrammed to iPSCs by virus containing pMXs-hSox2, pMXs-hOCT4, pMXs-hKlf4, pMXs-hc-Myc, and pCL-Eco (all from Addgene, Cambridge, MA, USA). The detailed procedures for viral packaging were the same as those described in a previous report.[7] In brief, HEK293T cells were seeded on six-well plates at a density of 80,000/cm^2. When confluence reached 80%, the cells were transfected with pMXs vectors (pMXs-hSox2, pMXs-hOCT4, pMXs-hKlf4, pMXs-hc-Myc, and pCL-Eco), using Lipofectamine 2000 (Invitrogen, Carlsbad, CA, USA); 2.5 μg of the pCL-Eco packaging vector and 2.5 μg of the corresponding pMXs vector were used per well. On the day before infection, renal tubular epithelial cells were seeded on six-well plates at a density of 6,000/cm^2 and infected with viral supernatants that were collected 48 and 72 h after transfection in the presence of 8 μg/mL polybrene (Sigma-Aldrich, Burlington, MA, USA). After incubated for 24 h at 37°C, 5% CO_2, the renal tubular epithelial cells were infected with viral supernatants for a second infection. Then, the cells were trypsinized and seeded at 100,000 cells per 10-cm dish containing feeders in ESC medium 4 days after infection. After 2 weeks, ESC-like clones were picked up and expanded for further characterization. All experimental protocols were approved by the Ethics Committee of the Center for Medical Genetics of Central South University, and the participant in this study provided and signed written informed consent. The N-iPSCs were purchased from ATCC (DYR0100, https://www.atcc.org/Products/All/ACS-1011.aspx).

Characterization of iPSCs

iPSC surface markers were identified by immunofluorescent staining. Cells were seeded on chamber slides and fixed in 4% paraformaldehyde for 15 min and then permeabilized with 0.1% Triton X-100 in DPBS for 15 min. The cells were blocked in 5% BSA for 30 min and then incubated with primary antibody diluted 1:100 in blocking buffer (OCT4; ab181557; Abcam), NANOG (ab109250; Abcam), SSEA-1 (SCR001; Merck Millipore), SSEA-4 (SCR001; Merck Millipore) at room temperature for 1 hour. After a thorough washing, the cells were blocked for 30 min again and then treated with secondary antibodies for 1 hour. Nuclei were stained with DAPI. Stained cells were photographed with a fluorescence microscope (Leica DM

IRB, Wetzlar, Germany). Teratoma formation experiments were performed to test the multilineage differentiation potential of the cells. Five million cells were dissociated with 0.05% trypsin/EDTA (Gibco, Grand Island, NY, USA), resuspended in 140 μL DMEM/F12 and 70 μL Matrigel (Corning, Corning, NY, USA) and injected into the groins of nude mice. The formed teratoma were harvested approximately 8 weeks later, fixed in 4% paraformaldehyde, embedded in paraffin, sectioned, and stained with H&E. All procedures regarding the care and use of animals were performed in accordance with institutional guidelines. All animal experiments were approved by the Institutional Animal Care and Use Committee of the Center for Medical Genetics of Central South University.

Karyotyping

After being treated with 0.1 μg/mL colcemid (Sigma-Aldrich, Burlington, MA) for 4 h, cells were trypsinized, pelleted, and incubated in 0.075 M KCl for 10 min at 37°C. After fixation with Carnoy fixative, metaphase chromosome spreads were prepared by using the air-drying method. The chromosomes were G-banded by Giemsa staining (Sigma-Aldrich) after appropriate baking at 75°C and digestion with trypsin.

Construction of CRISPR/Cas9 Plasmids and Detection of Cleavage Activity

Two sgRNAs were designed to target human *F8* exon 14 using Optimized CRISPR Design (http://zlab.bio/guide-design-resources/)[28] and then verified by using the CHOPCHOP website (http://chopchop.cbu.uib.no/)[60] and CRISPR RGEN tool (http://www.rgenome.net/cas-designer/).[61] The synthetic sgRNAs were synthesized by Sangon Biotech (Shanghai, China), then cloned into pX330, which was obtained from Feng Zhang's laboratory (Addgene No. 42230). Briefly, the complementary sgRNA oligos were annealed and then ligated with the *Bbs*I (New England Biolabs, Ipswich, MA, USA) digested plasmid using T4 DNA ligase (Thermo Fisher Scientific, Waltham, MA, USA). To detect cleavage activity, HA-iPSCs were nucleofected using Nucleofector II (Lonza) set at program B016 according to the manufacturer's instructions. Genomic DNA was extracted 48 h after transfection. The genomic region containing the targeting locus was amplified and cloned, and the construct was used to transform bacteria. For F8-E14-sg1, 46 colonies were picked and sequenced. For F8-E14-sg2, 37 clones were picked and sequenced. Gene disruption was also evaluated by the T7E1 assay. In brief, the PCR products were purified and digested with mismatch-sensitive T7E1. After electrophoresis, the cleaved and uncleaved fragments were quantified by using a gel imaging system.

Gene Targeting of the *F8* Locus in HA-iPSCs

HA-iPSCs cultured on Matrigel were detached with TrypLE Select (Life Technologies, Grand Island, NY, USA). The dissociated single cells were resuspended with 100 μL of Human Stem Cell Nucleofector Kit 2 (Lonza,) and nucleofected using Nucleofector II (Lonza) set at program B016. For 1×10^6 cells, 2.5 μg of each CRISPR/Cas9 plasmid was used, with or without 50 pmol ssODN synthesized by Sangon Biotech (Shanghai, China). The transfected cells were seeded on Matrigel-coated wells in mTeSR1 (Stem Cell Technologies, Vancouver, BC, Canada) containing 10 μM Y27632. After 2 days, the cells were detached with TrypLE Select (Life Technologies), and 10,000 cells were seeded on MEF feeders in ESC medium containing 10 μM Y27632 in a 100-mm culture dish.[62] Approximately 2 weeks later, clones were picked and expanded. To detect gene deletion events, DNA from individual colonies was extracted and subjected to PCR. PCR was performed using the primers F8-E14-forward (F): 5′-GGTGGACCTCTGAGCTTGAGTGA-3′ and F8-E14-reverse (R): 5′-GCATCTTAAAGAACGACATATCTGGAT-3′. The PCR products were identified by agarose gel electrophoresis. The 448-bp product was sequenced by Sanger sequencing.

Analysis of Off-Target Mutations Induced by CRISPR/Cas9

To analyze the off-target activity of CRISPR/Cas9, we used Sanger sequencing and WES for HA- and C-iPSCs. Genomic DNA of HA- and C-iPSCs (2-6- and 2-46-iPSCs) was isolated. For Sanger sequencing, the DNA from C-iPSCs (2-6- and 2-46-iPSCs) and HA-iPSCs were PCR amplified for five potential off-target sites for F8-E14-sg1 and F8-E14-sg2 predicted by the Optimized CRISPR Design website and sequenced; indels were used to evaluate off-target effects in C-iPSCs. For WES, genomic DNA isolated from HA-iPSCs and C-iPSCs were fragmented and ligated with adaptors to construct libraries, and then, the libraries were subjected to WES using Novaseq 6000 (Illumina, San Diego, CA, USA). The potential off-target sites of CRISPR/Cas9 were searched for by using Cas-OFFinder, which is accessible at http://www.rgenome.net.

Differentiation of hiPSC-Derived ECs

The differentiation of hiPSCs to ECs was carried out as previously described.[34] Briefly, hiPSCs were seeded on Matrigel with OP9-diff-conditioned medium (OP9-diff-CM). OP9-diff-CM was collected from the 5- to 10-day-old OP9 cells cultured with OP9-diff medium (α-MEM supplemented with 10% FBS and monothioglycerol; Sigma-Aldrich) and filtered. The medium was refreshed daily. On day 9, the differentiated cells were harvested and sorted with a CD31 MicroBead Kit (Miltenyi Biotec, Auburn, CA, USA) according to the manufacturer's instructions. The sorted ECs were characterized by immunostaining of endothelial markers CD31 and CD144. Primary antibodies against CD31 (P8590-.2ML; Sigma-Aldrich) and CD144 (ab33168; Abcam) were used.

Derivation of EPCs from hiPSCs

Human iPSCs were differentiated to EPCs via small-molecule-mediated activation of WNT signaling, as previously described.[35] Cells were dissociated with Accutase (Thermo Fisher Scientific) and seeded on Matrigel-coated cell culture wells at 50,000 cells/cm^2 in mTeSR1 containing 10 μM Y27632. Cells were cultured in mTeSR1 for 3 days and cultured in LaSR basal medium (Advanced/F12, 2.5 mM GlutaMAX and 60 mg/mL ascorbic acid; Sigma-Aldrich) supplemented with 6 μM CHIR99021 (Selleck Chemicals, Houston, TX, USA) for 2 days. After 2 days, the cells were maintained in LaSR basal medium without CHIR99021 for an additional 3 days. The cells were characterized by flow cytometry and an immunofluorescence assay.

The differentiated cells were sorted with a CD31 MicroBead Kit (Miltenyi Biotec) according to the manufacturer's instructions. Then the sorted EPCs were cultured on collagen IV-coated cell culture dishes (Corning) in endothelial growth medium (EGM-2; Lonza) for further differentiation to ECs.

RT-PCR

Total RNA was extracted with TRIzol reagent (Sigma-Aldrich) and treated with DNase for 30 min. Then the RNA was reverse transcribed using random primers and Oligo(dT)$_{15}$ (Vazyme, Nanjing, China). Two pairs of primers were used to detect the transcripts of *F8*. One primer was based on exon 14, which contained the deleted 54-bp fragment, and the other was based on exons 23 and 26. The glyceraldehyde-3-phosphate dehydrogenase (GAPDH) gene was amplified as an endogenous control. Primer sequences are shown in Table S1.

FVIII Assay of Culture Supernatants and Cell Lysates

The culture supernatants were harvested from 12-well plates 24 h after medium replacement. Then the cells were dissociated with Accutase and counted. After washing with DPBS, the pelleted cells were resuspended in 500 μL of sample diluent for ELISA (Cedarlane, Burlington, ON, Canada) and lysed by three freeze-thaw cycles. All samples were collected in triplicate. ELISA was performed using Paired Antibodies for ELISA-Factor VIII:C (Cedarlane, Burlington, ON, Canada) according to the manufacturer's instructions. Reference curves were constructed using serial dilutions of normal pooled plasma, with a correlation coefficient (R^2) of at least 0.990 using a semilog fit. For the FVIII activity assay, 24-hour-old cell-free supernatant was collected. To calculate FVIII activity, coagulation factor VIII-deficient plasma (Siemens Healthcare Diagnostics, Marburg, Germany) and a Destiny Max hemostasis analyzer (Tcoag, Lemgo, Germany) were used to examine the activated partial thromboplastin time (aPTT). All manipulations were performed according to the manufacturer's instructions.

Vascular Tube Formation and AcLDL Uptake

To evaluate the function of iECs, 5×10^4 iECs were plated on Matrigel-coated, 48-well culture plates with EGM-2 medium (Lonza). Tube formation was observed using light microscopy after 16 h of incubation.

For the AcLDL uptake assay, the iECs were washed twice with DPBS and then cultured in EGM-2 supplemented with 2.4 μg/mL DiI-AcLDL (Thermo Fisher Scientific) for 4 h at 37°C, washed with DPBS and observed using fluorescence microscopy.

Transplantation of iEPCs into HA Mice

The use and care of animals complied with the guidelines of the Ethics Committee of the Center for Medical Genetics of Central South University.

For *in vivo* transplantation, 6-week-old HA mice (strain: B6; 129S4-F8 tm1Kaz/J; Jackson Laboratory,)[63] were assigned equally in each group. And the same numbers of 6-week-old C57BL/6 mice were used as wild-type controls. The same number of males and females were in each group. Each mouse was anesthetized with Avertin (Sigma-Aldrich) and then infused with 2×10^6 iEPCs derived from HA-iPSCs, C-iPSCs (2-6-iPSCs and 2-46-iPSCs), or N-iPSCs by orbital vein injection. After transplantation, FK506 (1 mg/kg in 100 μL corn oil; Selleck Chemicals) treatment was performed via intraperitoneal injection once every other day. Two weeks after transplantation, a tail-clip challenge was carried out. Mice were anesthetized, and tail-clip assays were performed as previously described.[9] Briefly, the distal part of the mouse tail with a diameter of 1.5 mm was sheared and allowed to bleed for 5 min. The survival time was recorded after applying firm pressure on the tail for 1 minute. Tissue from the surviving mice was harvested and analyzed by using tissue immunofluorescence. Meanwhile, some mice were anesthetized, and blood samples were collected from their eyes to isolate plasma for the FVIII activity assay. All animal experiments were approved by the Institutional Animal Care and Use Committee of the Center for Medical Genetics of Central South University.

All of the mapped data are available from the SRA: SRP145757.

Statistical Analysis

Data were analyzed using ANOVA for more than two groups. The survival curve was analyzed with the log-rank test. All values in each group are presented as the mean ± SEM. All statistical analyses were performed using GraphPad Prism 5.0 software.

SUPPLEMENTAL INFORMATION

Supplemental Information can be found online at https://doi.org/10.1016/j.omtn.2019.05.019.

AUTHOR CONTRIBUTIONS

D.L. and L.W. designed and supervised the research and edited the manuscript. Z.H., M.Z., and Y.W. performed the experiments. Z.H. drafted the manuscript. M.Z. prepared the figures and edited the manuscript. Y.W., Z.L. and X.L. assisted in manuscript preparation. All authors read and approved the final manuscript.

CONFLICTS OF INTEREST

The authors declare no competing interests.

ACKNOWLEDGMENTS

We thank Wei Yin for feeding the animals, Ting Liang for the FVIII activity assay, Minyuan Peng for flow cytometry, and Yun Xie for biochemical detection. This work was supported by grants from the National Natural Science Foundation of China (31571313 and 81770200) and the National Key Research and Development Program of China (2016YFC0905102).

REFERENCES

1. Chuah, M.K., Nair, N., and VandenDriessche, T. (2012). Recent progress in gene therapy for hemophilia. Hum. Gene Ther. *23*, 557–565.

2. Stenson, P.D., Mort, M., Ball, E.V., Evans, K., Hayden, M., Heywood, S., Hussain, M., Phillips, A.D., and Cooper, D.N. (2017). The Human Gene Mutation

Database: towards a comprehensive repository of inherited mutation data for medical research, genetic diagnosis and next-generation sequencing studies. Hum. Genet. *136*, 665–677.

3. George, L.A., Sullivan, S.K., Giermasz, A., Rasko, J.E.J., Samelson-Jones, B.J., Ducore, J., Cuker, A., Sullivan, L.M., Majumdar, S., Teitel, J., et al. (2017). Hemophilia B Gene Therapy with a High-Specific-Activity Factor IX Variant. N. Engl. J. Med. *377*, 2215–2227.

4. McIntosh, J., Lenting, P.J., Rosales, C., Lee, D., Rabbanian, S., Raj, D., Patel, N., Tuddenham, E.G., Christophe, O.D., McVey, J.H., et al. (2013). Therapeutic levels of FVIII following a single peripheral vein administration of rAAV vector encoding a novel human factor VIII variant. Blood *121*, 3335–3344.

5. Rangarajan, S., Walsh, L., Lester, W., Perry, D., Madan, B., Laffan, M., Yu, H., Vettermann, C., Pierce, G.F., Wong, W.Y., and Pasi, K.J. (2017). AAV5-Factor VIII Gene Transfer in Severe Hemophilia A. N. Engl. J. Med. *377*, 2519–2530.

6. Chandler, R.J., Sands, M.S., and Venditti, C.P. (2017). Recombinant Adeno-Associated Viral Integration and Genotoxicity: Insights from Animal Models. Hum. Gene Ther. *28*, 314–322.

7. Wu, Y., Hu, Z., Li, Z., Pang, J., Feng, M., Hu, X., Wang, X., Lin-Peng, S., Liu, B., Chen, F., et al. (2016). In situ genetic correction of F8 intron 22 inversion in hemophilia A patient-specific iPSCs. Sci. Rep. *6*, 18865.

8. Park, C.Y., Kim, J., Kweon, J., Son, J.S., Lee, J.S., Yoo, J.E., Cho, S.R., Kim, J.H., Kim, J.S., and Kim, D.W. (2014). Targeted inversion and reversion of the blood coagulation factor 8 gene in human iPS cells using TALENs. Proc. Natl. Acad. Sci. USA *111*, 9253–9258.

9. Park, C.Y., Kim, D.H., Son, J.S., Sung, J.J., Lee, J., Bae, S., Kim, J.H., Kim, D.W., and Kim, J.S. (2015). Functional Correction of Large Factor VIII Gene Chromosomal Inversions in Hemophilia A Patient-Derived iPSCs Using CRISPR-Cas9. Cell Stem Cell *17*, 213–220.

10. Pang, J., Wu, Y., Li, Z., Hu, Z., Wang, X., Hu, X., Wang, X., Liu, X., Zhou, M., Liu, B., et al. (2016). Targeting of the human F8 at the multicopy rDNA locus in Hemophilia A patient-derived iPSCs using TALENickases. Biochem. Biophys. Res. Commun. *472*, 144–149.

11. Xiao, A., Wang, Z., Hu, Y., Wu, Y., Luo, Z., Yang, Z., Zu, Y., Li, W., Huang, P., Tong, X., et al. (2013). Chromosomal deletions and inversions mediated by TALENs and CRISPR/Cas in zebrafish. Nucleic Acids Res. *41*, e141.

12. Zuo, E., Huo, X., Yao, X., Hu, X., Sun, Y., Yin, J., He, B., Wang, X., Shi, L., Ping, J., et al. (2017). CRISPR/Cas9-mediated targeted chromosome elimination. Genome Biol. *18*, 224.

13. Blasco, R.B., Karaca, E., Ambrogio, C., Cheong, T.C., Karayol, E., Minero, V.G., Voena, C., and Chiarle, R. (2014). Simple and rapid in vivo generation of chromosomal rearrangements using CRISPR/Cas9 technology. Cell Rep. *9*, 1219–1227.

14. Maddalo, D., Manchado, E., Concepcion, C.P., Bonetti, C., Vidigal, J.A., Han, Y.C., Ogrodowski, P., Crippa, A., Rekhtman, N., de Stanchina, E., et al. (2014). In vivo engineering of oncogenic chromosomal rearrangements with the CRISPR/Cas9 system. Nature *516*, 423–427.

15. Wang, H., Yang, H., Shivalila, C.S., Dawlaty, M.M., Cheng, A.W., Zhang, F., and Jaenisch, R. (2013). One-step generation of mice carrying mutations in multiple genes by CRISPR/Cas-mediated genome engineering. Cell *153*, 910–918.

16. Yang, H., Wang, H., Shivalila, C.S., Cheng, A.W., Shi, L., and Jaenisch, R. (2013). One-step generation of mice carrying reporter and conditional alleles by CRISPR/Cas-mediated genome engineering. Cell *154*, 1370–1379.

17. Yoshimi, K., Kunihiro, Y., Kaneko, T., Nagahora, H., Voigt, B., and Mashimo, T. (2016). ssODN-mediated knock-in with CRISPR-Cas for large genomic regions in zygotes. Nat. Commun. *7*, 10431.

18. Rivera-Torres, N., and Kmiec, E.B. (2017). A Standard Methodology to Examine On-site Mutagenicity As a Function of Point Mutation Repair Catalyzed by CRISPR/Cas9 and SsODN in Human Cells. J. Vis. Exp. 56195.

19. Wang, X., Wang, Y., Huang, H., Chen, B., Chen, X., Hu, J., Chang, T., Lin, R.J., and Yee, J.K. (2014). Precise gene modification mediated by TALEN and single-stranded oligodeoxynucleotides in human cells. PLoS ONE *9*, e93575.

20. Fomin, M.E., Zhou, Y., Beyer, A.I., Publicover, J., Baron, J.L., and Muench, M.O. (2013). Production of factor VIII by human liver sinusoidal endothelial cells transplanted in immunodeficient uPA mice. PLoS ONE *8*, e77255.

21. Shahani, T., Covens, K., Lavend'homme, R., Jazouli, N., Sokal, E., Peerlinck, K., and Jacquemin, M. (2014). Human liver sinusoidal endothelial cells but not hepatocytes contain factor VIII. J. Thromb. Haemost. *12*, 36–42.

22. Wagner, D.D. (1993). The Weibel-Palade body: the storage granule for von Willebrand factor and P-selectin. Thromb. Haemost. *70*, 105–110.

23. Xu, D., Alipio, Z., Fink, L.M., Adcock, D.M., Yang, J., Ward, D.C., and Ma, Y. (2009). Phenotypic correction of murine hemophilia A using an iPS cell-based therapy. Proc. Natl. Acad. Sci. USA *106*, 808–813.

24. Zhou, T., Benda, C., Dunzinger, S., Huang, Y., Ho, J.C., Yang, J., Wang, Y., Zhang, Y., Zhuang, Q., Li, Y., et al. (2012). Generation of human induced pluripotent stem cells from urine samples. Nat. Protoc. *7*, 2080–2089.

25. Zhou, T., Benda, C., Duzinger, S., Huang, Y., Li, X., Li, Y., Guo, X., Cao, G., Chen, S., Hao, L., et al. (2011). Generation of induced pluripotent stem cells from urine. J. Am. Soc. Nephrol. *22*, 1221–1228.

26. Dörrenhaus, A., Müller, J.I., Golka, K., Jedrusik, P., Schulze, H., and Föllmann, W. (2000). Cultures of exfoliated epithelial cells from different locations of the human urinary tract and the renal tubular system. Arch. Toxicol. *74*, 618–626.

27. Takahashi, K., Tanabe, K., Ohnuki, M., Narita, M., Ichisaka, T., Tomoda, K., and Yamanaka, S. (2007). Induction of pluripotent stem cells from adult human fibroblasts by defined factors. Cell *131*, 861–872.

28. Hsu, P.D., Scott, D.A., Weinstein, J.A., Ran, F.A., Konermann, S., Agarwala, V., Li, Y., Fine, E.J., Wu, X., Shalem, O., et al. (2013). DNA targeting specificity of RNA-guided Cas9 nucleases. Nat. Biotechnol. *31*, 827–832.

29. Zimmermann, M.A., Oldenburg, J., Müller, C.R., and Rost, S. (2014). Expression studies of mutant factor VIII alleles with premature termination codons with regard to inhibitor formation. Haemophilia *20*, e215–e221.

30. Zheng, C., Liu, H.H., Yuan, S., Zhou, J., and Zhang, B. (2010). Molecular basis of LMAN1 in coordinating LMAN1-MCFD2 cargo receptor formation and ER-to-Golgi transport of FV/FVIII. Blood *116*, 5698–5706.

31. Kim, Y., Kweon, J., and Kim, J.S. (2013). TALENs and ZFNs are associated with different mutation signatures. Nat. Methods *10*, 185.

32. Bae, S., Park, J., and Kim, J.S. (2014). Cas-OFFinder: a fast and versatile algorithm that searches for potential off-target sites of Cas9 RNA-guided endonucleases. Bioinformatics *30*, 1473–1475.

33. Veres, A., Gosis, B.S., Ding, Q., Collins, R., Ragavendran, A., Brand, H., Erdin, S., Cowan, C.A., Talkowski, M.E., and Musunuru, K. (2014). Low incidence of off-target mutations in individual CRISPR-Cas9 and TALEN targeted human stem cell clones detected by whole-genome sequencing. Cell Stem Cell *15*, 27–30.

34. Hu, Z., Wu, Y., Zhou, M., Wang, X., Pang, J., Li, Z., Feng, M., Wang, Y., Hu, Q., Zhao, J., et al. (2018). Generation of reporter hESCs by targeting EGFP at the CD144 locus to facilitate the endothelial differentiation. Dev. Growth Differ. *60*, 205–215.

35. Lian, X., Bao, X., Al-Ahmad, A., Liu, J., Wu, Y., Dong, W., Dunn, K.K., Shusta, E.V., and Palecek, S.P. (2014). Efficient differentiation of human pluripotent stem cells to endothelial progenitors via small-molecule activation of WNT signaling. Stem Cell Reports *3*, 804–816.

36. Pipe, S.W. (2009). Functional roles of the factor VIII B domain. Haemophilia *15*, 1187–1196.

37. Pipe, S.W., Morris, J.A., Shah, J., and Kaufman, R.J. (1998). Differential interaction of coagulation factor VIII and factor V with protein chaperones calnexin and calreticulin. J. Biol. Chem. *273*, 8537–8544.

38. Cunningham, M.A., Pipe, S.W., Zhang, B., Hauri, H.P., Ginsburg, D., and Kaufman, R.J. (2003). LMAN1 is a molecular chaperone for the secretion of coagulation factor VIII. J. Thromb. Haemost. *1*, 2360–2367.

39. Miao, H.Z., Sirachainan, N., Palmer, L., Kucab, P., Cunningham, M.A., Kaufman, R.J., and Pipe, S.W. (2004). Bioengineering of coagulation factor VIII for improved secretion. Blood *103*, 3412–3419.

40. Zhang, B., Kaufman, R.J., and Ginsburg, D. (2005). LMAN1 and MCFD2 form a cargo receptor complex and interact with coagulation factor VIII in the early secretory pathway. J. Biol. Chem. *280*, 25881–25886.

41. Pittman, D.D., Alderman, E.M., Tomkinson, K.N., Wang, J.H., Giles, A.R., and Kaufman, R.J. (1993). Biochemical, immunological, and in vivo functional characterization of B-domain-deleted factor VIII. Blood *81*, 2925–2935.

42. Pittman, D.D., Marquette, K.A., and Kaufman, R.J. (1994). Role of the B domain for factor VIII and factor V expression and function. Blood *84*, 4214–4225.

43. Khrenov, A.V., Ananyeva, N.M., and Saenko, E.L. (2006). Role of the B domain in proteolytic inactivation of activated coagulation factor VIII by activated protein C and activated factor X. Blood Coagul. Fibrinolysis *17*, 379–388.

44. Bovenschen, N., Rijken, D.C., Havekes, L.M., van Vlijmen, B.J., and Mertens, K. (2005). The B domain of coagulation factor VIII interacts with the asialoglycoprotein receptor. J. Thromb. Haemost. *3*, 1257–1265.

45. Gringeri, A., Tagliaferri, A., Tagariello, G., Morfini, M., Santagostino, E., and Mannucci, P.; ReFacto-AICE Study Group (2004). Efficacy and inhibitor development in previously treated patients with haemophilia A switched to a B domain-deleted recombinant factor VIII. Br. J. Haematol. *126*, 398–404.

46. Lusher, J.M., and Roth, D.A. (2005). The safety and efficacy of B-domain deleted recombinant factor VIII concentrates in patients with severe haemophilia A: an update. Haemophilia *11*, 292–293.

47. Ishiwata, A., Mimuro, J., Kashiwakura, Y., Niimura, M., Takano, K., Ohmori, T., Madoiwa, S., Mizukami, H., Okada, T., Naka, H., et al. (2006). Phenotype correction of hemophilia A mice with adeno-associated virus vectors carrying the B domain-deleted canine factor VIII gene. Thromb. Res. *118*, 627–635.

48. Brown, H.C., Wright, J.F., Zhou, S., Lytle, A.M., Shields, J.E., Spencer, H.T., and Doering, C.B. (2014). Bioengineered coagulation factor VIII enables long-term correction of murine hemophilia A following liver-directed adeno-associated viral vector delivery. Mol. Ther. Methods Clin. Dev. *1*, 14036.

49. Benkert, P., Biasini, M., and Schwede, T. (2011). Toward the estimation of the absolute quality of individual protein structure models. Bioinformatics *27*, 343–350.

50. Waterhouse, A., Bertoni, M., Bienert, S., Studer, G., Tauriello, G., Gumienny, R., Heer, F.T., de Beer, T.A.P., Rempfer, C., Bordoli, L., et al. (2018). SWISS-MODEL: homology modelling of protein structures and complexes. Nucleic Acids Res. *46* (W1), W296–W303.

51. Ryu, S.-M., Koo, T., Kim, K., Lim, K., Baek, G., Kim, S.-T., Kim, H.S., Kim, D.-e., Lee, H., Chung, E., and Kim, J.-S. (2018). Adenine base editing in mouse embryos and an adult mouse model of Duchenne muscular dystrophy. Nat. Biotechnol. *36*, 536–539.

52. Zhou, M., Hu, Z., Qiu, L., Zhou, T., Feng, M., Hu, Q., Zeng, B., Li, Z., Sun, Q., Wu, Y., et al. (2018). Seamless Genetic Conversion of SMN2 to SMN1 via CRISPR/Cpf1 and Single-Stranded Oligodeoxynucleotides in Spinal Muscular Atrophy Patient-Specific Induced Pluripotent Stem Cells. Hum. Gene Ther. *29*, 1252–1263.

53. Young, C.S., Hicks, M.R., Ermolova, N.V., Nakano, H., Jan, M., Younesi, S., Karumbayaram, S., Kumagai-Cresse, C., Wang, D., Zack, J.A., et al. (2016). A Single CRISPR-Cas9 Deletion Strategy that Targets the Majority of DMD Patients Restores Dystrophin Function in hiPSC-Derived Muscle Cells. Cell Stem Cell *18*, 533–540.

54. Zhang, Y., Long, C., Li, H., McAnally, J.R., Baskin, K.K., Shelton, J.M., Bassel-Duby, R., and Olson, E.N. (2017). CRISPR-Cpf1 correction of muscular dystrophy mutations in human cardiomyocytes and mice. Sci. Adv. *3*, e1602814.

55. Follenzi, A., Benten, D., Novikoff, P., Faulkner, L., Raut, S., and Gupta, S. (2008). Transplanted endothelial cells repopulate the liver endothelium and correct the phenotype of hemophilia A mice. J. Clin. Invest. *118*, 935–945.

56. Corselli, M., Parodi, A., Mogni, M., Sessarego, N., Kunkl, A., Dagna-Bricarelli, F., Ibatici, A., Pozzi, S., Bacigalupo, A., Frassoni, F., and Piaggio, G. (2008). Clinical scale ex vivo expansion of cord blood-derived outgrowth endothelial progenitor cells is associated with high incidence of karyotype aberrations. Exp. Hematol. *36*, 340–349.

57. Eldesoqi, K., Henrich, D., El-Kady, A.M., Arbid, M.S., Abd El-Hady, B.M., Marzi, I., and Seebach, C. (2014). Safety evaluation of a bioglass-polylactic acid composite scaffold seeded with progenitor cells in a rat skull critical-size bone defect. PLoS ONE *9*, e87642.

58. Qin, M., Guan, X., Wang, H., Zhang, Y., Shen, B., Zhang, Q., Dai, W., Ma, Y., and Jiang, Y. (2017). An effective ex-vivo approach for inducing endothelial progenitor cells from umbilical cord blood $CD34^+$ cells. Stem Cell Res. Ther. *8*, 25.

59. Sharma, R., Anguela, X.M., Doyon, Y., Wechsler, T., DeKelver, R.C., Sproul, S., Paschon, D.E., Miller, J.C., Davidson, R.J., Shivak, D., et al. (2015). In vivo genome editing of the albumin locus as a platform for protein replacement therapy. Blood *126*, 1777–1784.

60. Montague, T.G., Cruz, J.M., Gagnon, J.A., Church, G.M., and Valen, E. (2014). CHOPCHOP: a CRISPR/Cas9 and TALEN web tool for genome editing. Nucleic Acids Res. *42*, W401–W407.

61. Park, J., Bae, S., and Kim, J.S. (2015). Cas-Designer: a web-based tool for choice of CRISPR-Cas9 target sites. Bioinformatics *31*, 4014–4016.

62. Tang, Z.H., Chen, J.R., Zheng, J., Shi, H.S., Ding, J., Qian, X.D., Zhang, C., Chen, J.L., Wang, C.C., Li, L., et al. (2016). Genetic Correction of Induced Pluripotent Stem Cells From a Deaf Patient With MYO7A Mutation Results in Morphologic and Functional Recovery of the Derived Hair Cell-Like Cells. Stem Cells Transl. Med. *5*, 561–571.

63. Bi, L., Lawler, A.M., Antonarakis, S.E., High, K.A., Gearhart, J.D., and Kazazian, H.H., Jr. (1995). Targeted disruption of the mouse factor VIII gene produces a model of haemophilia A. Nat. Genet. *10*, 119–121.

OMTN, Volume *17*

Supplemental Information

ssODN-Mediated In-Frame Deletion with CRISPR/Cas9 Restores FVIII Function in Hemophilia A-Patient-Derived iPSCs and ECs

Zhiqing Hu, Miaojin Zhou, Yong Wu, Zhuo Li, Xionghao Liu, Lingqian Wu, and Desheng Liang

Supplemental Figures and Legends

Figure S1

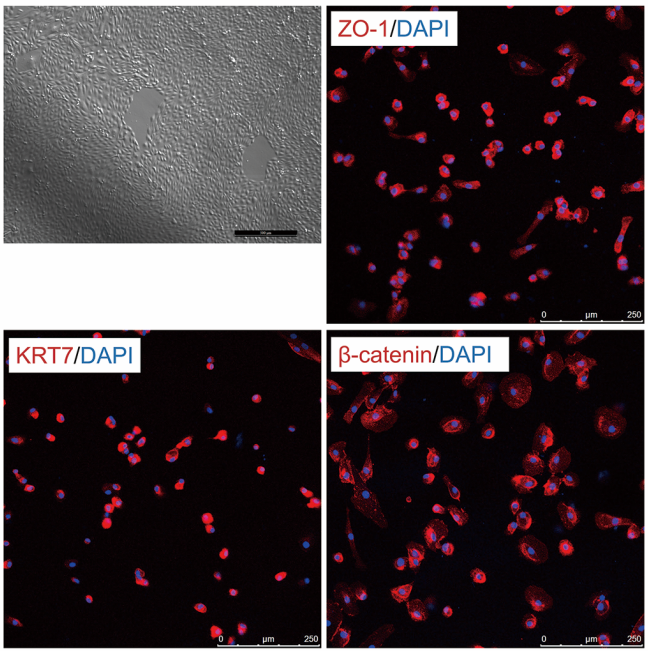

Figure S1. related to Figure 1

Morphology of the renal tubular epithelial cells and immunostaining of ZO-1, KRT7 and β-catenin, and 4',6'-diamidino-2-phenylindole (DAPI) for nuclear staining.

Figure S2

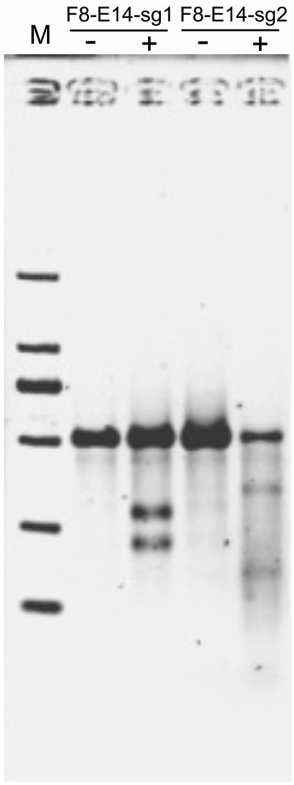

Figure S2. related to Figure 2

The cleavage efficiency of F8-E14-sgRNA1 and F8-E14-sgRNA2 in HA-iPSCs were detected by T7E1 assay.

Figure S3

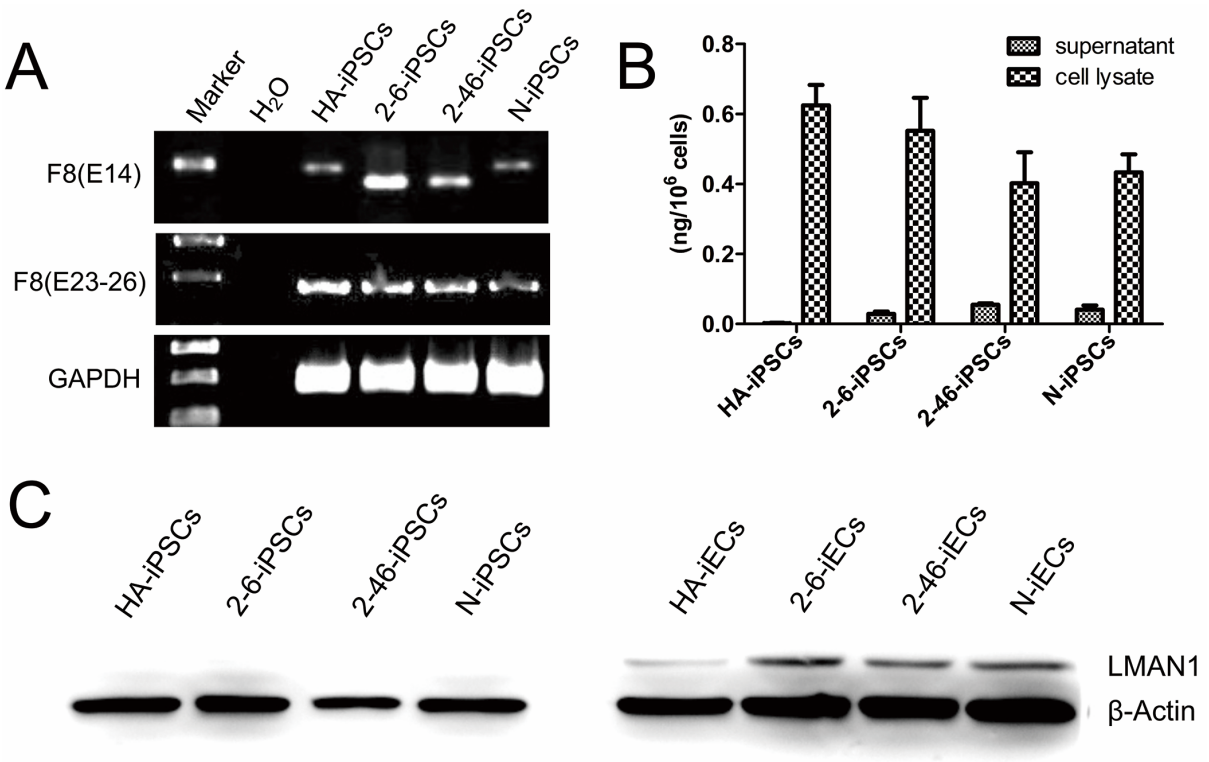

Figure S3. F8 expression at the iPSCs stage, related to Figure 2

(A) F8 transcription was analyzed by RT-PCR. The water (H_2O) was used as the blank control, HA-iPSCs was the patient group, 2-6-iPSCs and 2-46-iPSCs were the gene corrected clones, N-iPSCs was used as the normal control, GAPDH was used as the internal reference, and F8 (E14) was amplified for the gene fragment deletion region, F8 (E23-26) was amplified from exon 23 to exon 26. (B) ELISA detection of FVIII concentrations of cell lysate and cell culture supernatant at iPSC stage. Bars represent the mean ± SEM (n=3, independent cultures). (C) Western blot analysis of LMAN1 protein in iPSCs and iECs. β-Actin was used as the internal reference.

Figure S4

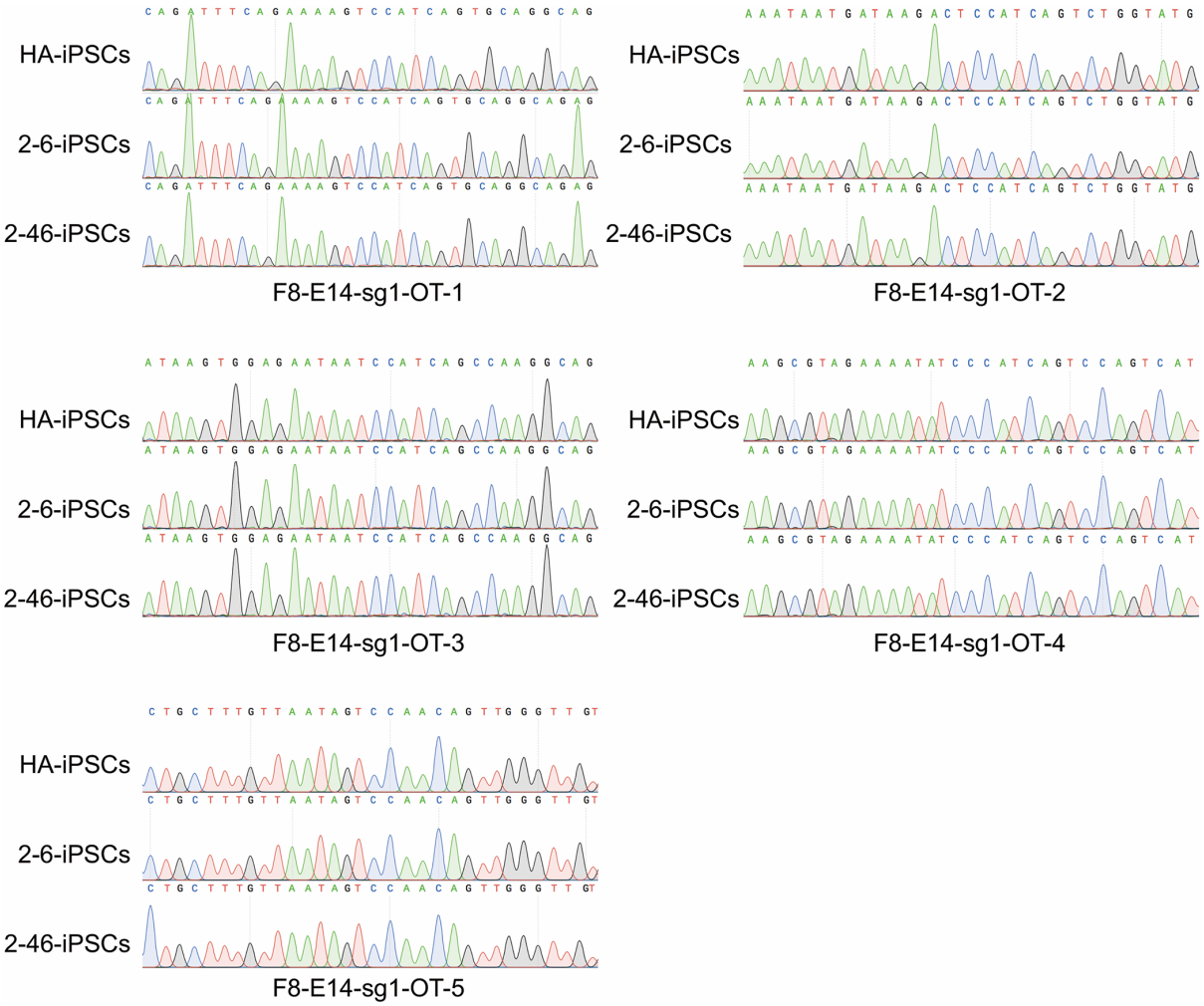

Figure S4. **Sanger sequencing of the five potential off-target sites after reframed using F8-E14-sg1, related to Table 1 and Table S3 and S5**

The HA-iPSCs and the corrected clones 2-6-iPSCs and 2-46-iPSCs were analyzed. No indels were found at the sites.

Figure S5

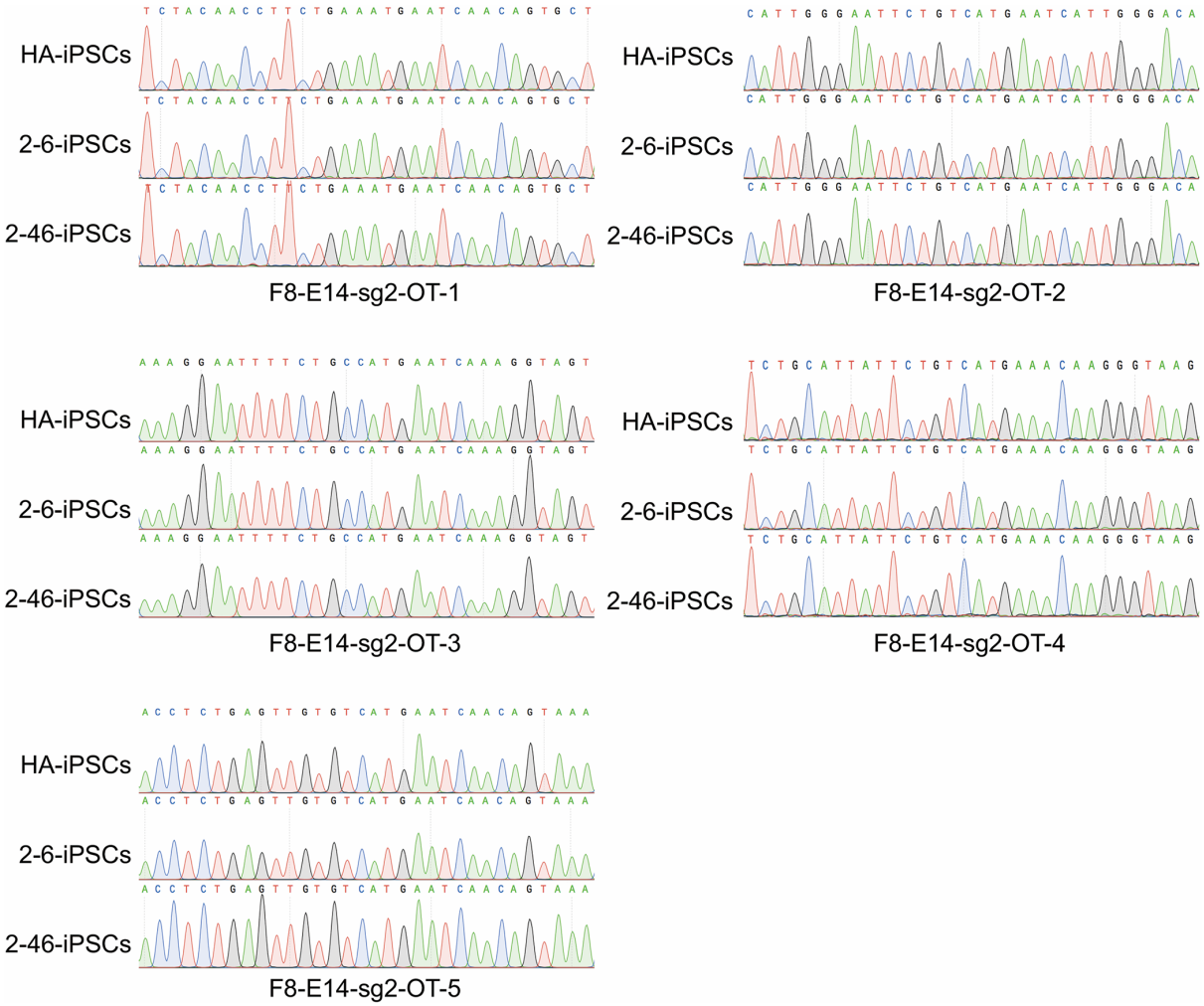

Figure S5. **Sanger sequencing of the five potential off-target sites after reframed using F8-E14-sg2, related to Table 1 and Table S4 and S5**

The HA-iPSCs and the corrected clones 2-6-iPSCs and 2-46-iPSCs were analyzed. No indels were found at the sites.

Figure S6

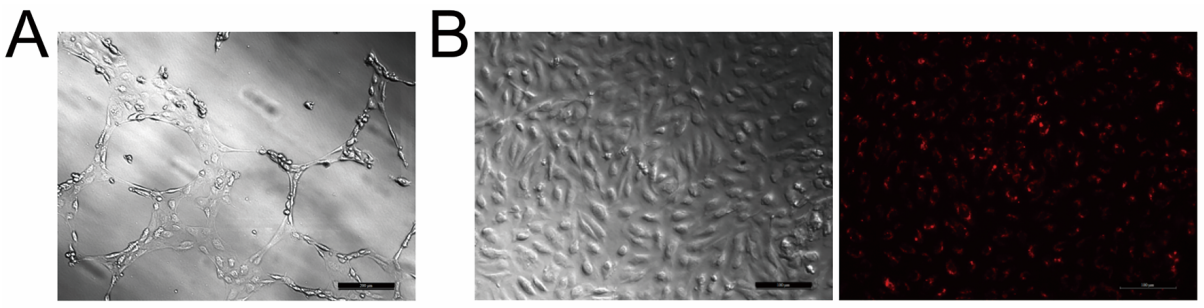

Figure S6. *In vitro* detection of iPSCs-derived endothelial cells function, related to Figure 4

(A) Angiogenesis assay of endothelial cells. (B) Dil-acLDL endocytosis in endothelial cells. The red fluorescence signal was endocytic Dil-acLDL.

Supplemental tables

Table S1. Primers used in genotyping and RT-PCR, related to Figure 2

Primer name	Sequence (5' to 3')	Used for the experiment of
F8-14-g1-F	CACCGTGAGAATAGTCCATCAGTC	Construction of sgRNA1
F8-14-g1-R	AAACGACTGATGGACTATTCTCAC	
F8-14-g2-F	CACCGGCATTCTGTCATGAATCAA	Construction of sgRNA2
F8-14-g2-R	AAACTTGATTCATGACAGAATGCC	
F8-E14-F	GGTGGACCTCTGAGCTTGAGTGA	PCR for reframed clones screening and RT-PCR for F8-Exon 14
F8-E14-R	GCATCTTAAAGAACGACATATCTGGAT	
GAPDH-F	GGGGAGCCAAAAGGGTCATCATCT	RT-PCR for GAPDH
GAPDH-R	GACGCCTGCTTCACCACCTTCTTG	
F8-RT-E23F	CACTCTTCGCATGGAGTTGA	RT-PCR for F8-E23-26
F8-RT-E26R	GGGGGTGAATTCGAAGGTAG	
ssODN	CATTGATGGCCCATCATTATTAATTGAGAATAGTCCATCAA TTCATGACAGAATGCTTATGGACAAAAATGCTACAGCTT	ssODN for gene targeting

Table S2. Summary of the experiments of targeted gene deletion, related to Figure 2

Experiment group	Total analysis Clone	Reframed HA-iPS clone	Targeting efficiency
F8-E14-sg1/F8-E14-sg2 with ssODN	34	5	5/34=14.71%
F8-E14-sg1/F8-E14-sg2	48	1	1/48=2.08%

Table S3. Potential off-target sites of F8-E14-sg1 predicted by the Optimized CRISPR Design web, related to Figure 2 and Figure S4

sequence	score	mismatches	UCSC gene	locus
TTCAGAAAAGTCCATCAGTGCAG	1.4	3MMs[3:8:20]		chr6:-116338171
ATGATAAGACTCCATCAGTCTGG	1.3	4MMs[1:5:8:10]		chr3:-121903943
TGGAGAATAATCCATCAGCCAAG	1.0	3MMs[2:10:19]		chr1:-175915498
TAGAAAATATCCCATCAGTCCAG	0.7	4MMs[2:5:10:11]	NM_001369	chr5:+13817688
TTGTTAATAGTCCAACAGTTGGG	0.2	4MMs[4:5:15:20]	NM_138395	chr2:+198572468

Five off-target sites predicted by the Optimized CRISPR Design web. The mismatch is indicated by colored letters.

Table S4. Potential off-target sites of F8-E14-sg2 predicted by the Optimized CRISPR Design web, related to Figure 2 and Figure S5

sequence	score	mismatches	UCSC gene	locus
AACCTTCTGAAATGAATCAACAG	0.7	4MMs[2:4:10:11]	NM_001257273	chr6:-56970352
GGAATTCTGTCATGAATCATTGG	1.5	3MMs[1:3:20]		chr17:+73212269
AATTTTCTGCCATGAATCAAAGG	1.3	4MMs[2:3:4:10]		chr4:+183813406
ATTATTCTGTCATGAAACAAGGG	1.2	3MMs[2:3:17]		chr3:+16296679
TGAGTTGTGTCATGAATCAACAG	0.9	4MMs[1:3:4:7]		chr13:+52418308

Five off-target sites predicted by the Optimized CRISPR Design web. The mismatch is indicated by colored letters.

Table S5. Primers used in CRISPR/Cas9 off-target analysis, related to Figure S4 and Figure S5

Site	Forward primer	Reverse primer	Expected product size, bp
F8-E14-sg1-OT-1	TTTGGTTGCTCAAAACTTGG	AGAAAGCCTGAAACAGTGCC	416
F8-E14-sg1-OT-2	GCTGTCTTGGGAACTTTGCT	CCCTGAGGACCACCTTGTGA	419
F8-E14-sg1-OT-3	GAACTTTCTAAACAAAACACCCT	ATGCTGGCAATCCCAATT	552
F8-E14-sg1-OT-4	TCGGGAAATGAGGATGAAT	AAAAATAGGCTGTACTTAAATGAGA	499
F8-E14-sg1-OT-5	TCAGGTGCCTGCTCCTATT	ATTCCGAATCCTCAATCTTTA	510
F8-E14-sg2-OT-1	TTGCTGGTGGTATTTATGTGAA	TGAAAGAGTTTATGCTCCCTTC	553
F8-E14-sg2-OT-2	AACCACGGGAAGTCGTTAGA	CCTGGGCAACAAGAGTGAA	366
F8-E14-sg2-OT-3	AAAGTAGCCTGCCAGATTGAA	TACACTGAGCTGTATCCCTAATGAC	543
F8-E14-sg2-OT-4	TTTTGAGTTTCCAGAAGCAGAG	ATCACTGTCTTCTTCCCTCCA	484
F8-E14-sg2-OT-5	GTAGGTATGCGATAACCTCCACT	CATTTTTAATAGTCATGGCTGGA	579